Naval Research Laboratory

Washington, DC 20375-5320

NRL/MR/7100--14-9578

Hypothetical Mine Hunting Sonar — Internal Wave Impact on Performance

Stewart M. Simpson

U.S. Naval Academy
Annapolis, Maryland

Marshall H. Orr

The University of Delaware
Newark, Delaware

Edward Tucholski

U.S. Naval Academy
Annapolis, Maryland

December 9, 2014

REPORT DOCUMENTATION PAGE

Form Approved
OMB No. 0704-0188

1. REPORT DATE *(DD-MM-YYYY)*
09-12-2014

2. REPORT TYPE
Memorandum Report

3. DATES COVERED *(From - To)*

4. TITLE AND SUBTITLE
Hypothetical Mine Hunting Sonar – Internal Wave Impact on Performance

5a. CONTRACT NUMBER

5b. GRANT NUMBER

5c. PROGRAM ELEMENT NUMBER

6. AUTHOR(S)
Stewart M. Simpson,[1] Marshall H. Orr,[2] and Edward Tucholski[1]

5d. PROJECT NUMBER

5e. TASK NUMBER

5f. WORK UNIT NUMBER

7. PERFORMING ORGANIZATION NAME(S) AND ADDRESS(ES)
Naval Research Laboratory, Code 7100
4555 Overlook Avenue, SW
Washington, DC 20375-5350

8. PERFORMING ORGANIZATION REPORT NUMBER
NRL/MR/7100--14-9578

9. SPONSORING / MONITORING AGENCY NAME(S) AND ADDRESS(ES)
Naval Research Laboratory, Code 7100
4555 Overlook Avenue, SW
Washington, DC 20375-5350

10. SPONSOR / MONITOR'S ACRONYM(S)

11. SPONSOR / MONITOR'S REPORT NUMBER(S)

12. DISTRIBUTION / AVAILABILITY STATEMENT
Approved for public release; distribution is unlimited.

13. SUPPLEMENTARY NOTES
[1]U.S. Naval Academy, Physics Department, 572C Holloway Road, Annapolis, MD 21402
[2]The University of Delaware, The College of Earth, Ocean and Environment, 111 Robinson Hall, Newark, DE 19716. The research reported here was performed while the author was employed in the Acoustics Division, Naval Research Laboratory.
*Enclosed DVD contains supplemental material

14. ABSTRACT
Acoustic signals exhibit continuous spatial and temporal variability when propagating through a sound speed field that is perturbed by oceanic internal waves. Acoustic systems operating in an internal wave perturbed sound speed field will exhibit performance variability. Numerical simulations are presented which quantify the impact of oceanic internal waves on the performance of a hypothetical mine hunting sonar system operating near a continental shelf break. The simulations show that signal excess probability distributions vary with target depth and range and the variability in the performance of the sonar system will be dependent on the figure of merit parameters selected for the system's operation.

15. SUBJECT TERMS
Mine hunting sonar performance   Stratified water column
Oceanic internal waves   Fall conditions

16. SECURITY CLASSIFICATION OF:			17. LIMITATION OF ABSTRACT	18. NUMBER OF PAGES	19a. NAME OF RESPONSIBLE PERSON
a. REPORT	b. ABSTRACT	c. THIS PAGE			Douglas G. Todoroff
Unclassified Unlimited	Unclassified Unlimited	Unclassified Unlimited	Unclassified Unlimited	25	19b. TELEPHONE NUMBER *(include area code)* (202) 767-3482

Standard Form 298 (Rev. 8-98)
Prescribed by ANSI Std. Z39.18

I. Introduction

Mine hunting sonar systems may be operated on continental shelves in sound speed fields that are perturbed by a variety of fluid dynamic processes including propagating internal wave groups[1]. The development of optimal deployment and search strategies for systems operating in such environments requires a quantitative understanding of their performance variability. Calculations have been performed to quantify the performance variability of a mine hunting sonar projecting signals parallel to the propagation vector of an internal wave group generated near a continental shelf break. They were done using a range and time dependent sound speed field synthesized from experimental data acquired in the early fall of 2000 on the New Jersey USA shelf during the NRL/ONR Shallow Water Acoustic Technology (SWAT) experiment. The calculations were done by placing a hypothetical mine hunting sonar system source at a fixed depth within the water column and moving a 4.5 km long internal wave field perturbed sound speed field through a mine field in discrete steps. The time dependent variability of acoustic signal incident on each target in the mine field was calculated for a selected acoustic source depth. The targets were placed at a number of ranges and depths within the water column and on the ocean bottom. The Navy Standard Comprehensive Acoustic System Simulation / Gaussian Ray Bundle (CASS/GRAB) computer program[2], was used to calculate both the variability of the intensity of the acoustic signal incident on each target and the acoustic field transmission loss variability.

Manuscript approved August 18, 2014

The computational approach is overviewed in Section II. The results of the calculations are presented in Section III and conclusions concerning the operational relevance of internal wave perturbation of the sound field are discussed in section IV.

II. Computational Approach

We estimated an internal wave field's impact on a mine hunting sonar's performance variability by: 1. creating a range/time dependent sound speed field using ocean measurements, 2. propagating acoustic signal through the generated sound speed field using CASS/GRAB, 3. extracting the intensity variability of acoustic signals incident on targets at a number of ranges and depths, 4. estimating the magnitude of acoustic signal scattered from the targets and received by a mine hunting sonar operating a fixed depth and 5. calculating the signal excess (***SE***) variability at the mine hunting sonar for a defined system figure of merit (***FOM***). The implementation of each of the five listed items is outlined. The hypothetical mine hunting sonar used a single 20 kHz transducer array operating in a backscattering mode, i.e. source and receiver arrays are at the same point in space.

Sound Speed Field Generation

Conductivity and temperature data versus depth (CTD) and time acquired on the New Jersey Shelf from October 3, 2000 22:28:28 Zulu, to OCT 4, 2000, 1:57:08 Zulu was used to generate a range dependent sound speed field. The data was taken as several mode one internal waves passed beneath the research vessel (R/V) *Endeavor* which was moored in ~ 68 m deep water, see green marker B in Figure 1. The data was acquired with a CTD instrument package that was raised and lowered vertically through the water column with a winch. A high frequency acoustic backscattering system was used to visualize the fluid processes occurring in the water column as the CTD was lowered and raised. A simple schematic of the data collection setup is shown in Figure 2.

Figure 1: Location of R/V *Endeavor*[3] during moored CTD operations (Lat: 39.34˚, Long: -72.88˚).

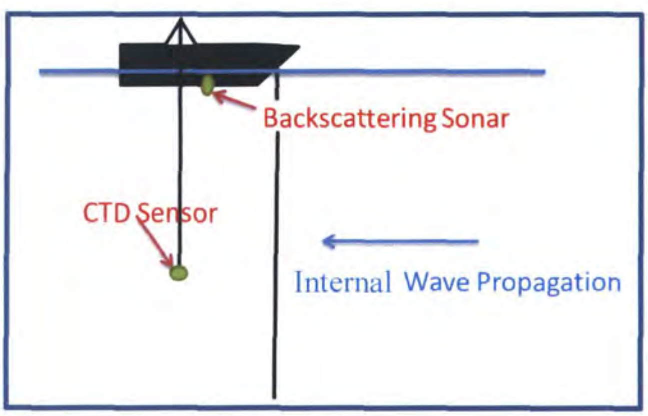

Figure 2: Data Collection Setup. The CTD was raised and lowered to measure the conductivity and temperature variability as a function of depth and time. A backscattering sonar was used to

image fluid processes. The blue arrow indicates the propagation direction of a mode 1 internal wave field.

Data from twenty CTD casts were used to construct a sound speed field. The data was taken during a ~ 200 minute time internal. Each CTD cast generated two independent sound velocity profiles, one on the down cast, and one on the up cast, for a total of forty independent profiles. The sound speed field was composed of two nearly constant sound speed layers separated by a strong sound speed gradient near mid water depth, see Figure 3.

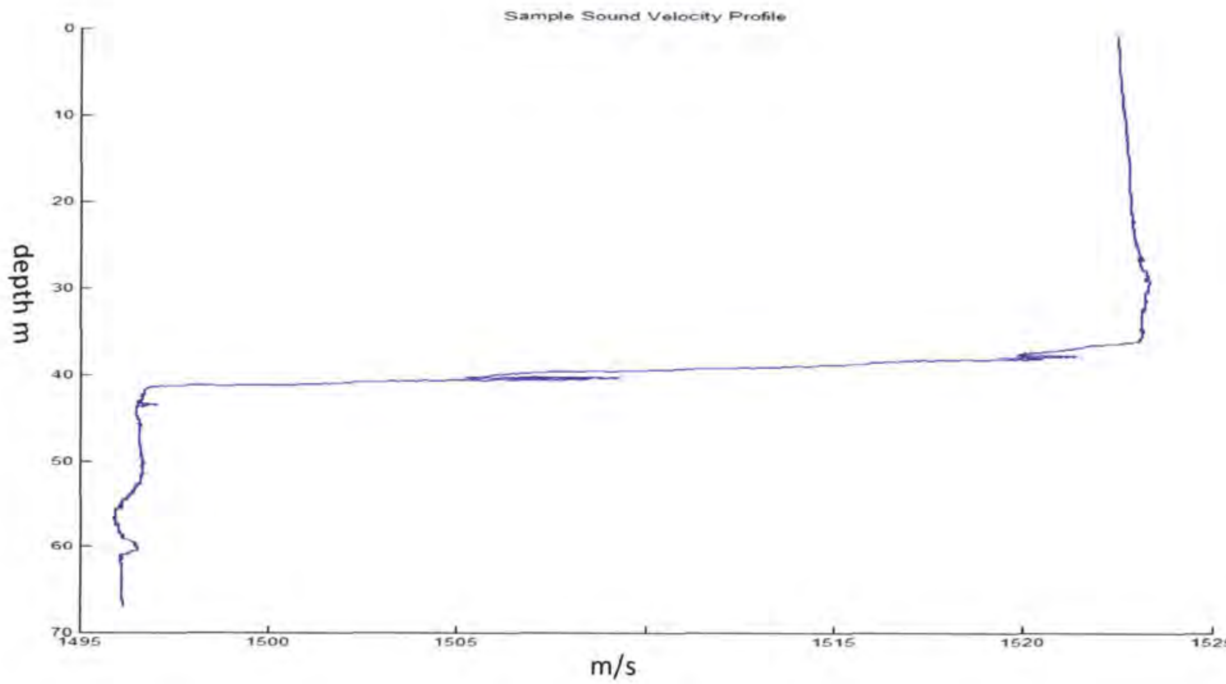

Figure 3: Sample sound velocity profile, X-axis (m/s), Y-axis (m)

During the CTD data acquisition period a 200 kHz high frequency acoustic backscattering sonar imaged the water column using acoustic signals scattered from neutrally buoyant acoustic impedance variability (particles, temperature and salinity gradients and velocity fluctuations).

The sonar imaged mode 1 internal wave vertical displacement of the neutrally buoyant scatters as the internal waves propagated through the water column beneath the ship, see Figure 4. In the following discussions, the vertical displacement of the acoustic scattering layers will be correlated to the temporal displacement of the sound speed field by the passing internal wave field. The V like structure in Figure 4 is caused by acoustic signal backscattering from the CTD sensor package as it was lowered and raised through the water column. It is clear from the acoustic image that the CTD sampling of the water column was temporally aliased.

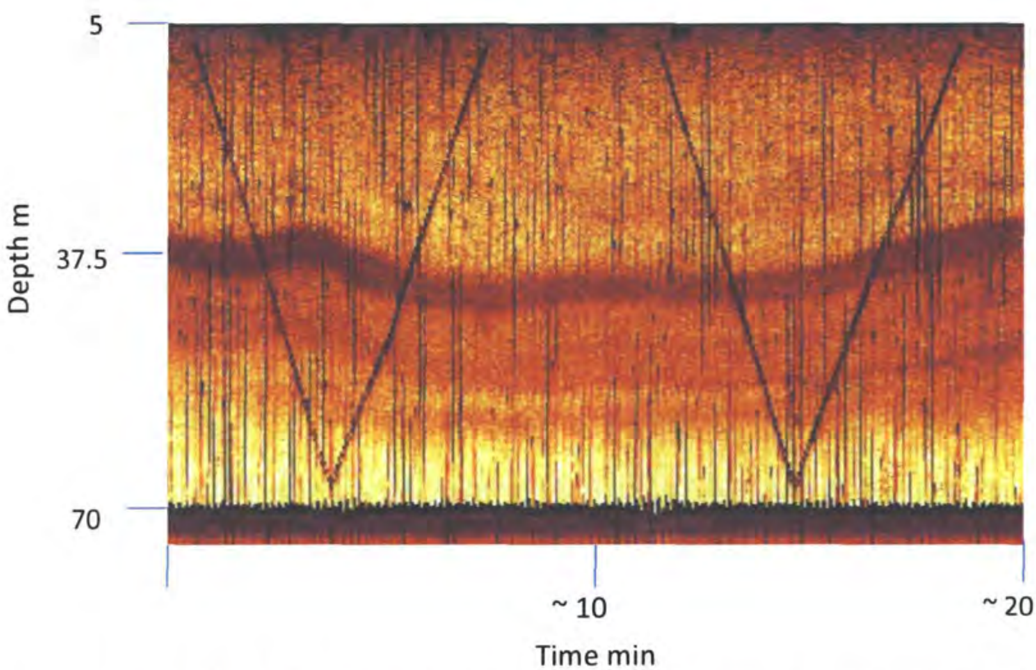

Figure 4: Acoustic backscatter image of a mode 1 internal wave displacement of the pycnocline. The Y-axis is depth (5 – 70 m) and the X-axis is time. The length of the record is about 20 min.

The CTD and acoustic data taken during the 200 min time interval was converted to a range dependent sound speed field by: 1. "merging" the CTD and acoustic backscatter data sets and 2.

converting the time record of the internal wave displacement of the sound speed field to a space record by multiplying the time by the internal wave propagation speed of 0.4 m/s. A 4.5 km long internal wave perturbed sound speed field was generated from the 40 time separated sound speed profiles.

The procedure used to merge the aliased CTD data and the backscattered acoustic image data is outlined. Each up and down segment of a CTD cast, although distributed in time, was treated as though it was acquired instantaneously at a specific time point. The down segment of the cast was assigned a time point about half way between the start of cast and the termination of the cast. The up segment was assigned a time point at the termination of the cast.

Separately, a Triton Elics International Inc. Isis Sonar software package was used to digitize selected acoustical scattering layers in five second steps to obtain the scattering layer depth dependence as a function of time. The acoustic scattering layer was correlated with a sound speed by noting when the CTD down or up cast crossed the scattering layer depth. The two data sets were then merged when the sound speed correlated with the acoustic scattering layer was plotted between the down and up segment of each CTD casts. The process resulted in a continuously varying range and depth dependent sound speed profile that incorporated the 40 CTD measurements.

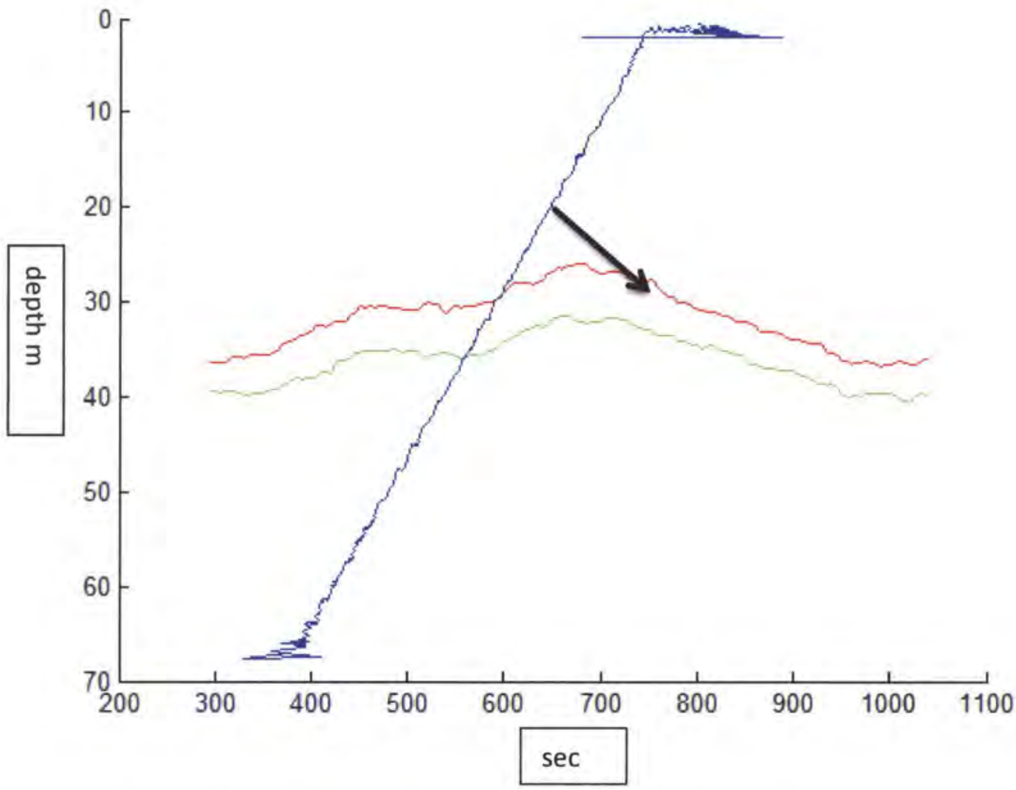

Figure 5: Calibration Example, Blue line CTD cast, red and green line digitized acoustic backscattering layers.

In detail, the red and green lines in Figure **5** are a section of the digitized acoustic scattering layers. The blue line shows the depth of the CTD as a function of time. The sound speed measured at the depth the CTD intercepted the acoustic scattering layer depth was assigned to the scattering layer (isosound speed layer). The red and green scattering layers were observed to be in phase for the 200 minutes of data analyzed, i.e. the internal waves were mode 1 in nature. Consequently, the red scattering layer displacement was arbitrarily selected to interpolate the isosound speed vertical displacements between each cast's up and down components.

The isosound speed lines digitization interval is 25 sec intervals in time or 10 m steps in space. The first 2500 seconds of the generated sound velocity profile is displayed in Figure 6.

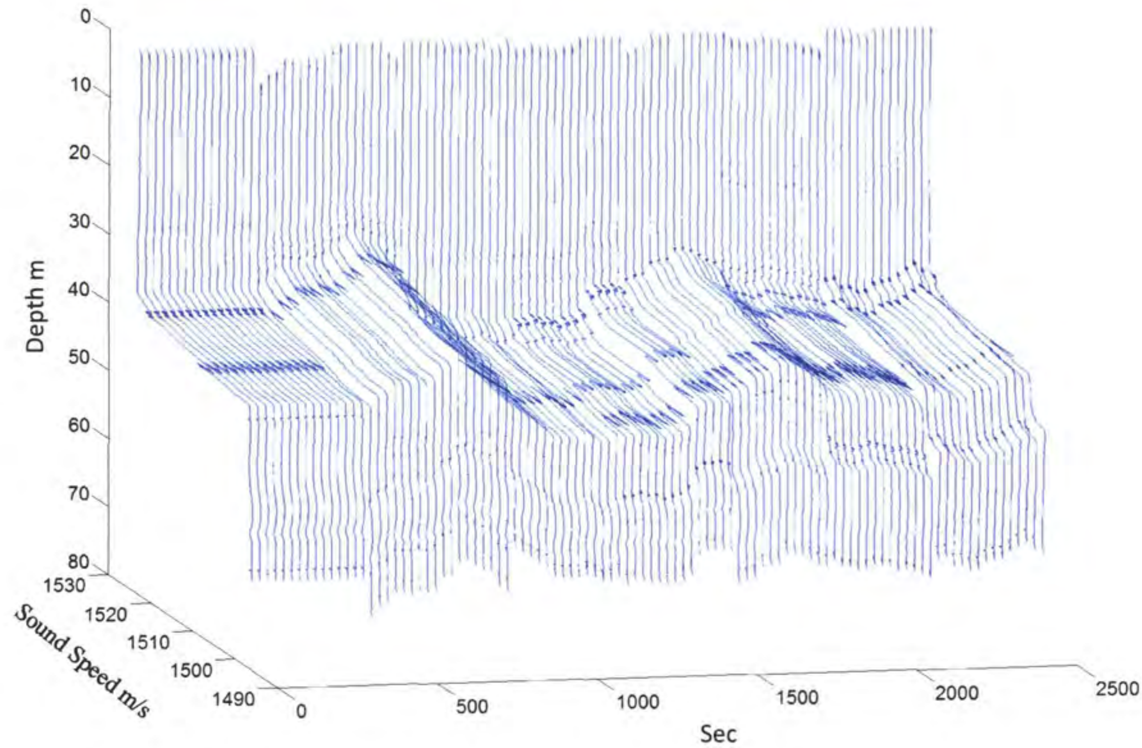

Figure 6: Example of generated range-dependent profile. X-axis (m/s), Y-axis (s), Z-axis (m)

The time dependent sound speed profile was converted to a range dependent sound speed profile by assuming the internal wave group propagation speed was 0.4 m/s. Consequently, Figure 6 presents a 1000 m long section of an internal wave displaced sound speed field. The ~ 4.5 km range dependent sound speed field generated from the ~ 200 min of CTD data was used as the sound speed field in the CASS/GRAB ray trace[4] acoustic propagation calculations described next. It temporal variability of the sound speed profile during a 83.3 minute time interval is shown in the power point file burned to the attached DVD.

Acoustic Signal Propagation Simulation

As indicated, the acoustic signal propagation calculations were made with the Navy Standard Comprehensive Acoustic System Simulation / Gaussian Ray Bundle (CASS/GRAB) ray trace computer program. The mine hunting sonar source was placed at a fixed location and depth at the beginning of the 4.5 km sound speed field. Spherical targets were placed at 100, 200, 400 and 800 m from the acoustic signal source and at 25, 35, 45, 60 and 70 depths, see stars in Figure 8a and b. Acoustic signals were propagated from the mine hunting system to a range of 1000 m. The acoustic signal strength and transmission loss at each of the target were extracted. The sound speed field was then moved to the left by 10 m (25 sec time steps) to simulate the propagation of the internal wave field through the mine field. Again the transmission loss and acoustic signal strength were extracted and stored. These calculations were repeated 200 times. The CASS/GRAB calculations environmental input parameters were set for a calm surface with a wind speed of two meters per second and a flat sandy bottom.

The acoustic signal propagation calculations were done for a stationary sonar system deployed at depth of twenty and fifty meters. The sonar system pinged every twenty-five seconds and operated at 20 kHz. The transducer beam pattern was a fan directed 15 degrees up from the horizontal and 5 degrees down from the horizontal. A MatLab script executed the CASS/GRAB software package. An illustrative example of CASS/GRAB's ray-trace output is displayed in Figure 7. The transmission loss to each of the targets changed as the sound speed profile moved through the mine field, see Figure 8a and 8b for a representative transmission loss calculation.

Two videos in the Power Point presentation contained in the attached DVD show the variability of the transmission loss for two sonar operating depths (20 and 50 m) as an internal wave group propagates through the target field at 0.45 m/s. The videos are for a 83.3 minute time interval, i.e. 200 frames with 25 sec between each frame. The following discussion will focus on the 50 m source depth calculations. Note that in the case of a submarine moving through a spatially distributed mine field placed in a moving internal wave field the calculations will have to be altered to reflect the changing sound speed field and changing range of the mine hunting sonar to targets.

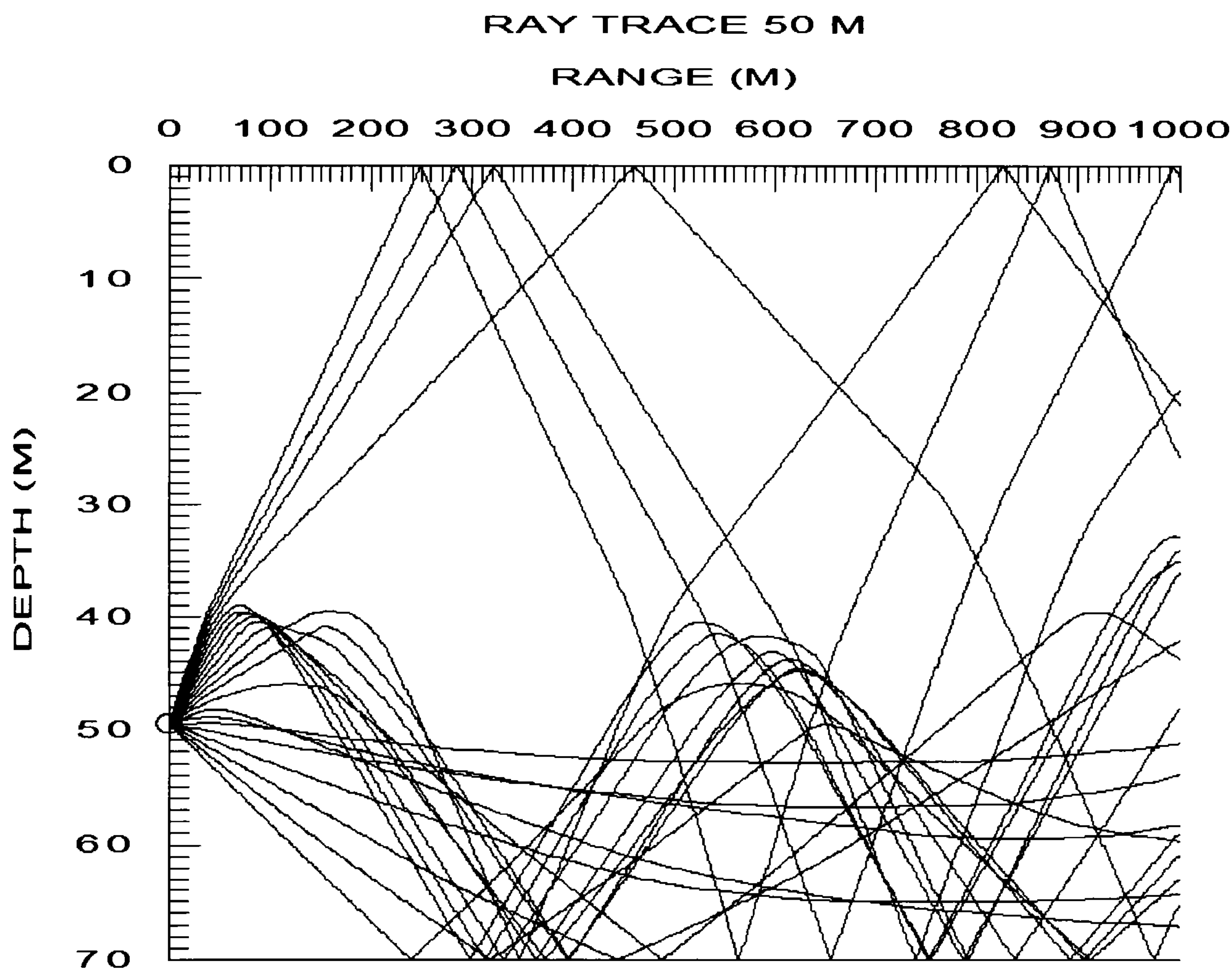

Figure 7: An illustrative ray-trace output from CASS/GRAB. The source is at 50 m

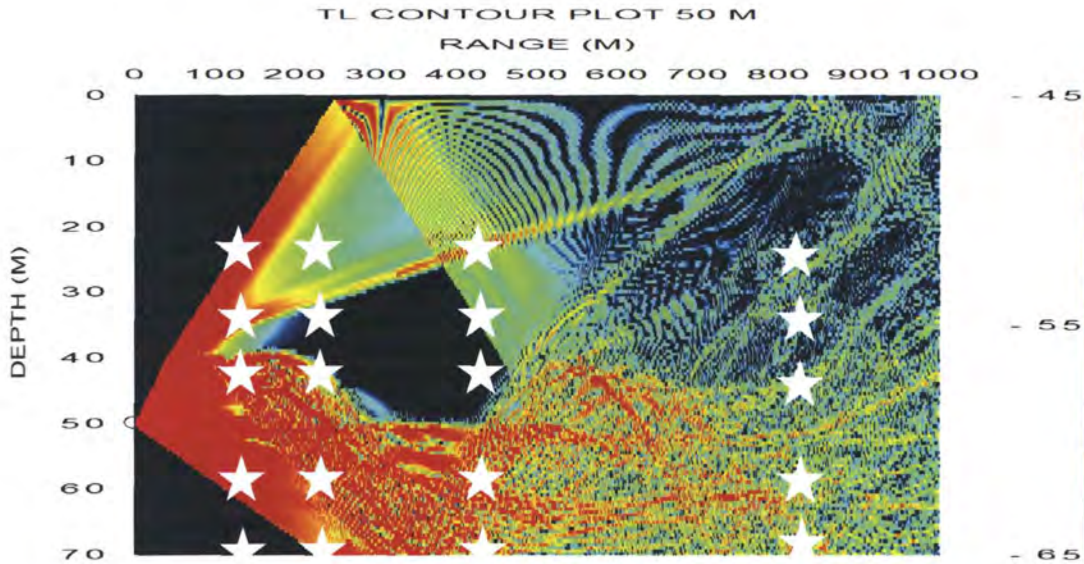

Figure 8a: A contour transmission loss plot for a 20 kHz projector placed at 50 m. Target depth is noted by the white stars. The color scale is in decibels.

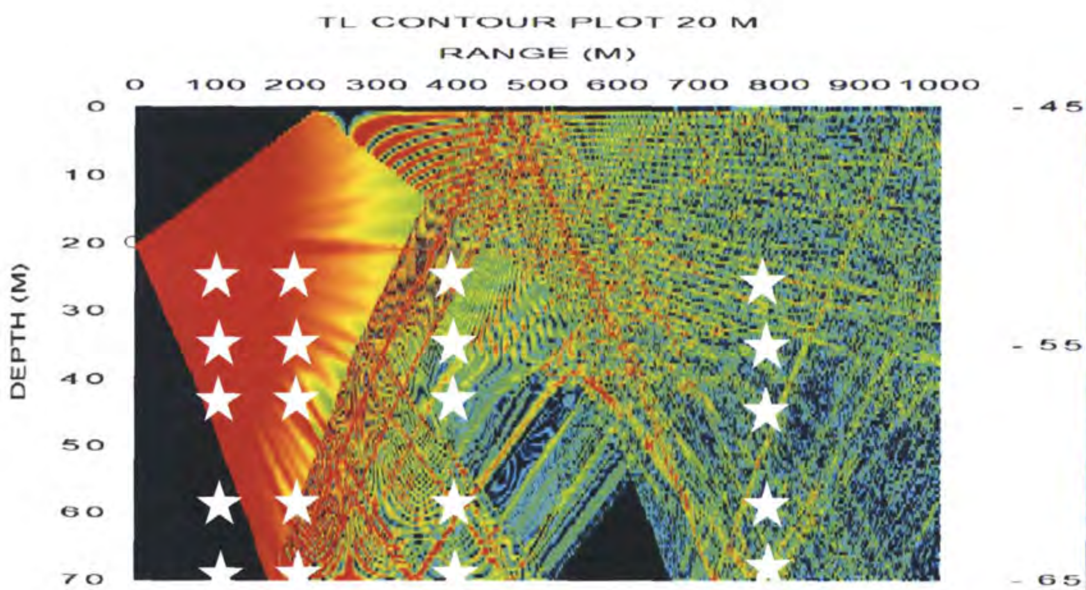

Figure 9b: A contour transmission loss plot for a 20 kHz projector placed at 20 m. Target depth is noted by the white stars. The color scale is in decibels.

The Mine Hunting Sonar Performance

The temporal variability of the performance of the mine hunting sonar system operating in a range and time dependent internal wave perturbed sound speed profile was evaluated by calculating the temporal variability of the signal excess (***SE***) of acoustic signals back scattered from targets distributed through the water column and on the bottom, see Figure 8a and b.

The *SE* is defined as the difference between the sonar system's figure of merit (*FOM*) and two times the one way transmission loss (*TL*). It is expressed as:

$$\boldsymbol{SE = FOM - 2TL} \qquad 1)$$

where *FOM* = figure of merit and *TL* = transmission loss. The calculation assumes the ocean is frozen during each ping's propagation time, from the acoustic source to a target of interest and along the return path from the target to the receiving hydrophone.

The *FOM* is defined as:

$$FOM = SL + TS - DT - NL + DI \qquad 2)$$

where SL= Source Level; TS= Target Strength; DT= Detection Threshold; NL= Noise Level and DI=Directivity Index.

A *FOM* of 174 dB was used to calculate the *SE* for each sound speed field realization. The *FOM* was calculated using a *DT* of 20 dB, a source level (*SL*) of 240 dB re 1μPa @ 1m, a target strength (*TS*) of -6 dB, a transducer *DI* of 18 dB and a reverberation noise level (*NL*) of 58 dB. The reverberation noise level is of the same magnitude as that measured at 20 kHz during ~ 10 m/s wind events. Note the CASS/GRAB calculation was done for a wind speed of ~ 1 m/s. The variability of the *FOM* and *SE* as a function of source level is plotted in Figure 8c. The *SE* has been plotted for a *TL* of 55 and 65 dB.

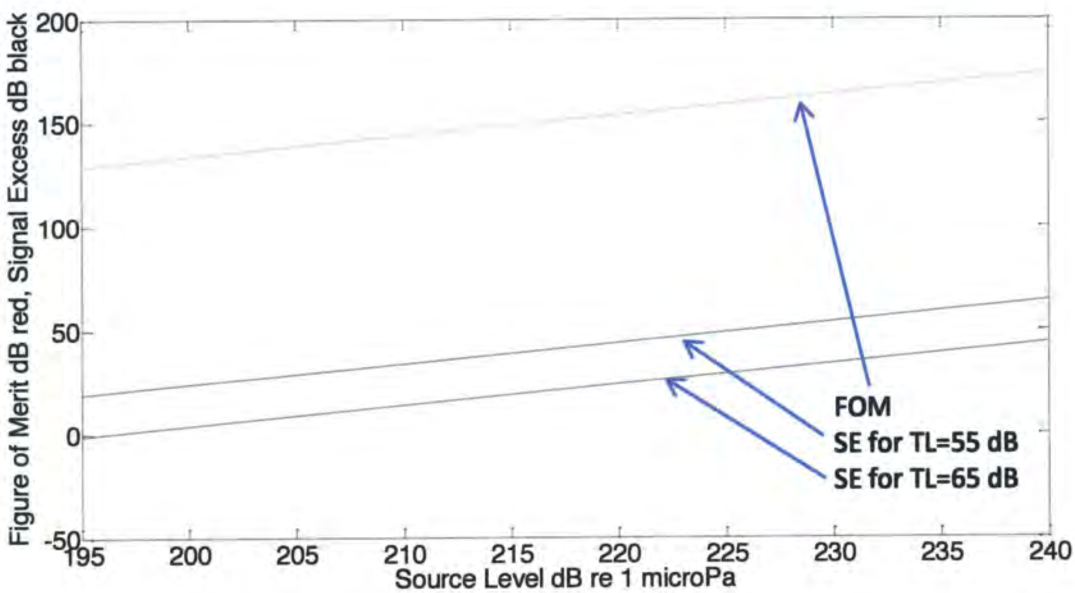

Figure 8c: Figure of merit (red) for the parameters listed in the text. Signal excess (black) for a transmission loss of 55 (upper curve) and 65 dB (lower curve) are plotted as a function of source level.

III. **Results**

The *SE* variability versus time caused by the internal wave perturbation of the sound speed field is plotted on the left of the Figures 9-13 for a source depth of 50 m, and spherical targets placed at 25, 35, 45, 60 and 70 m depths at ranges of 100, 200, 400 and 800 m from the sonar system. Note the targets at 70 m were on the bottom. Only *SE* greater than zero were plotted. A histogram of the *SE* variability distribution is plotted in the right column. The histogram is the probability distribution of the mine hunting sonars performance variability. The distribution was not fitted to an analytic probability distribution because of the range and depth variability seen in the figures and the limited temporal extent of the internal wave perturbed sound field used in the simulations.

The *SE* for the target at 25 m depth shows only a few detections with *SE* => 0 at a range of 100 m, and nearly continuous detections with *SE* => 0 at the 200, 400 and 800 m range points, see Figure 9. Comparing both the *SE* variability versus time and the histogram of the *SE* variability shows that the magnitude or breadth of the variability increases with increasing range for the target at 25 m depth. The *TL* plot for one time instance in Figure 8a shows the 25 m depth target to be outside the beam pattern at 100 m range and inside the beam pattern at the other ranges. This is reflected in the range dependence of the SE. The impact of the increasing average transmission loss on the *SE* with range is seen as a movement of the SE distribution patterns to smaller average values with increasing range. It is clear that the histograms or probability distribution for detecting the target changes with range.

The percentage of the projected signals that resulted in a *SE* greater than zero dB for each target depth and range versus changing *FOM* is listed in Table I. In the case of the 25 m deep target and a *FOM* of 174 dB, the number of detections was 1, 98.5, 91.5 and 98 % for the 100, 200, 400 and 800 m ranges respectively during the 1.38 hour simulation time interval. If the signal source level is decreased in 20 dB steps (for instance decreasing source level to minimize counter detection) the percentage of detections for the 25 m deep target with range decreased as the number of detections with *SE* greater than 0 decreases, see Table I. For a 60 dB decrease in source level the number of detections went from 1, 97.5, 57.5 and 20.5 % for the 100, 200, 400 and 800 m ranges respectively during the 1.38 hour simulation time interval. The mine hunting sonar performance was compromised as its performance effectiveness was changed due to the internal wave induce variability of the SE.

Inter-comparison of *SE* variability for the in water targets at depth 35, 45 and 60 m, see Figure 9 through 12 shows similar characteristics in the *SE* variability as that noted for the target at 25 m. The histograms, i.e. probability distributions of the *SE*, as a function of target depth and range were all different. In general they were spread over a greater SE span of values with increasing range ranging from ~ 20 dB at short ranges to greater than 60 dB at the longer ranges. As noted in Table I the performance of the system for each of the target depths was degraded due to the internal wave perturbation of the sound speed field and the SE.

Table I

	% SE > 0	% SE > 0	% SE > 0	% SE > 0
FOM	174	154	134	114
TLM25100	1	1	1	1
TLM25200	98.5	98.5	98.5	97.5
TLM25400	91.5	91.5	86.5	57.5
TLM25800	98	96	84.5	20.5
TLM35100	99.5	99.5	99.5	99.5
TLM35200	99.5	99.5	99.5	86
TLM35400	81	79.5	66	34.5
TLM35800	99.5	96.5	85.5	35
TLM45100	100	100	100	99.5
TLM45200	100	100	100	88
TLM45400	94	94	88.5	63.5
TLM45800	100	99.5	94.5	62.5
TLM60100	9	9	8.5	8.5
TLM60200	100	100	100	99.5
TLM60400	100	100	100	90.5
TLM60800	100	99.5	93.5	61
TLM70100	0	0	0	0
TLM70200	35.5	34	23	11.5
TLM70400	100	99.5	98.5	82.5
TLM70800	100	98.5	95	57.5

Table I: The first column lists the depth and range of the target from the mine hunting sonar transducer, i.e. TLM25100 stands for target depth of 25 m target range of 100 m.

Target Depth 25 m

Source Depth 50 m

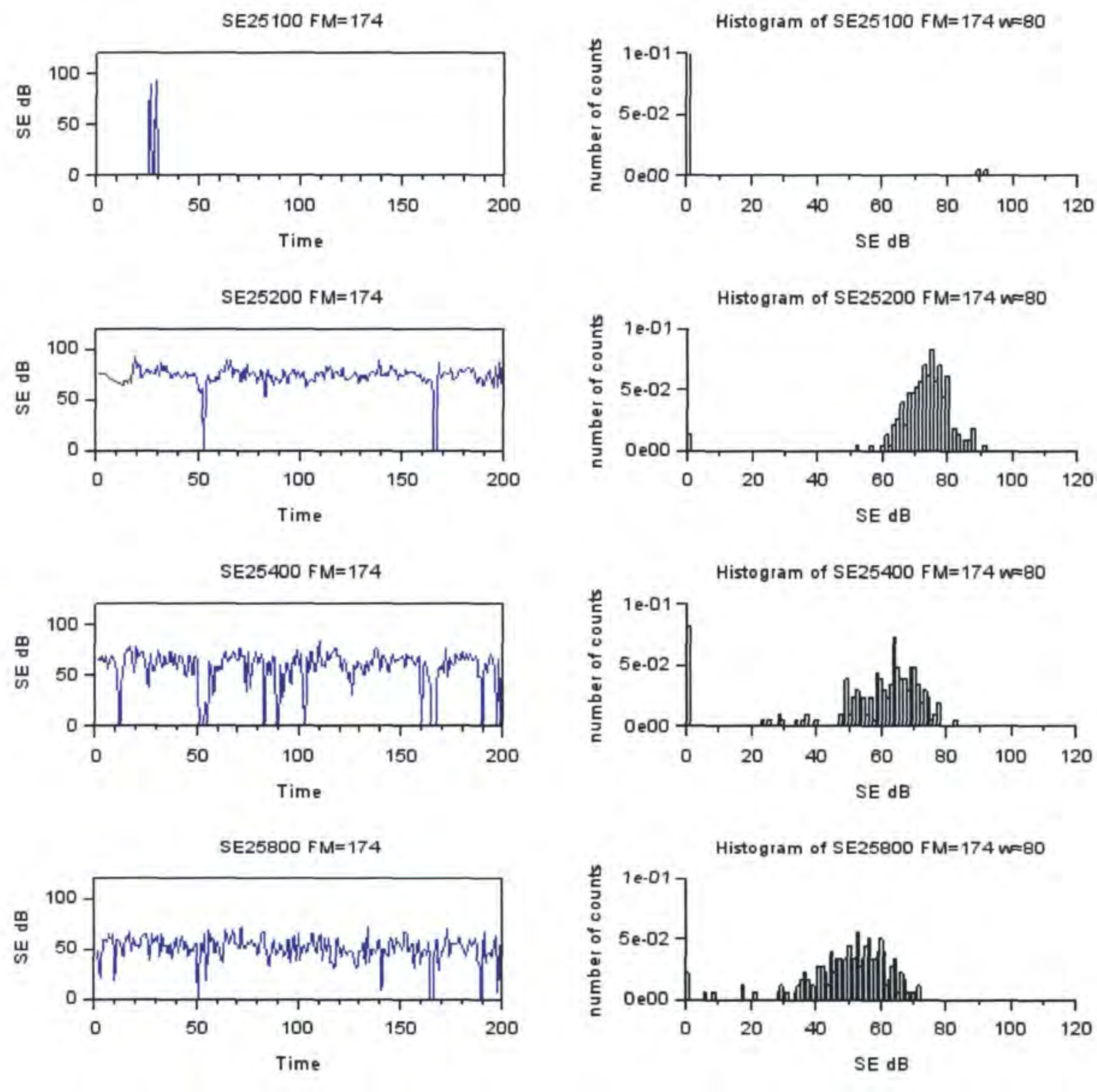

Figure 9. Left Column: Signal Excess (SE) for a target at 25 m depth and source at 50 m depth for 100 m, 200 m, 400 m and 800 m ranges. Right column histogram of SE for the same ranges. FM is the Figure of Merit.

Target Depth 35 m

Source Depth 50 m

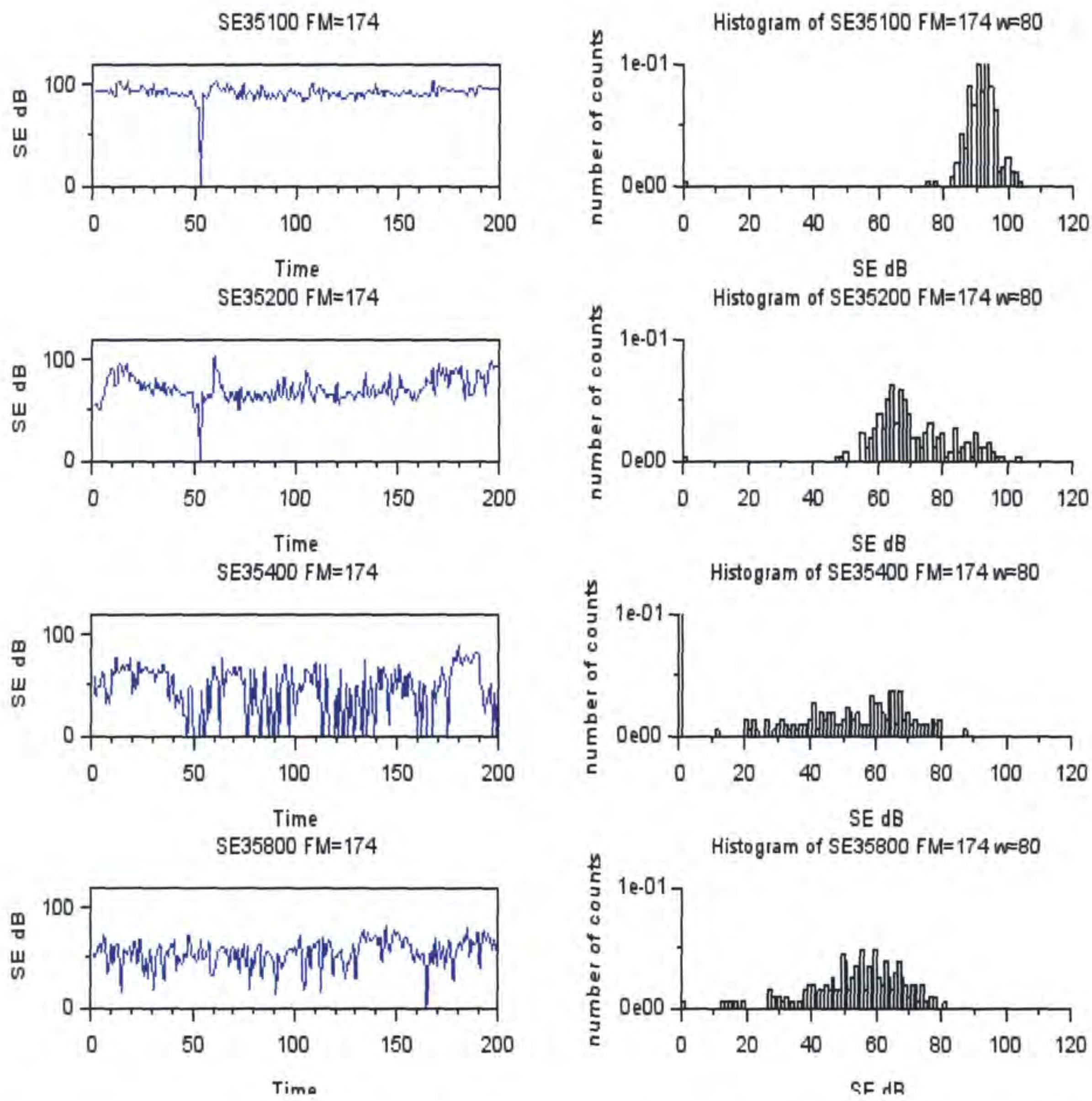

Figure 10. Left Column: Signal Excess (SE) for a target at 35 m depth and source at 50 m depth for 100 m, 200 m, 400 m and 800 m ranges. Right column histogram of SE for the same ranges. FM is the Figure of Merit.

Target Depth 45 m

Source Depth 50 m

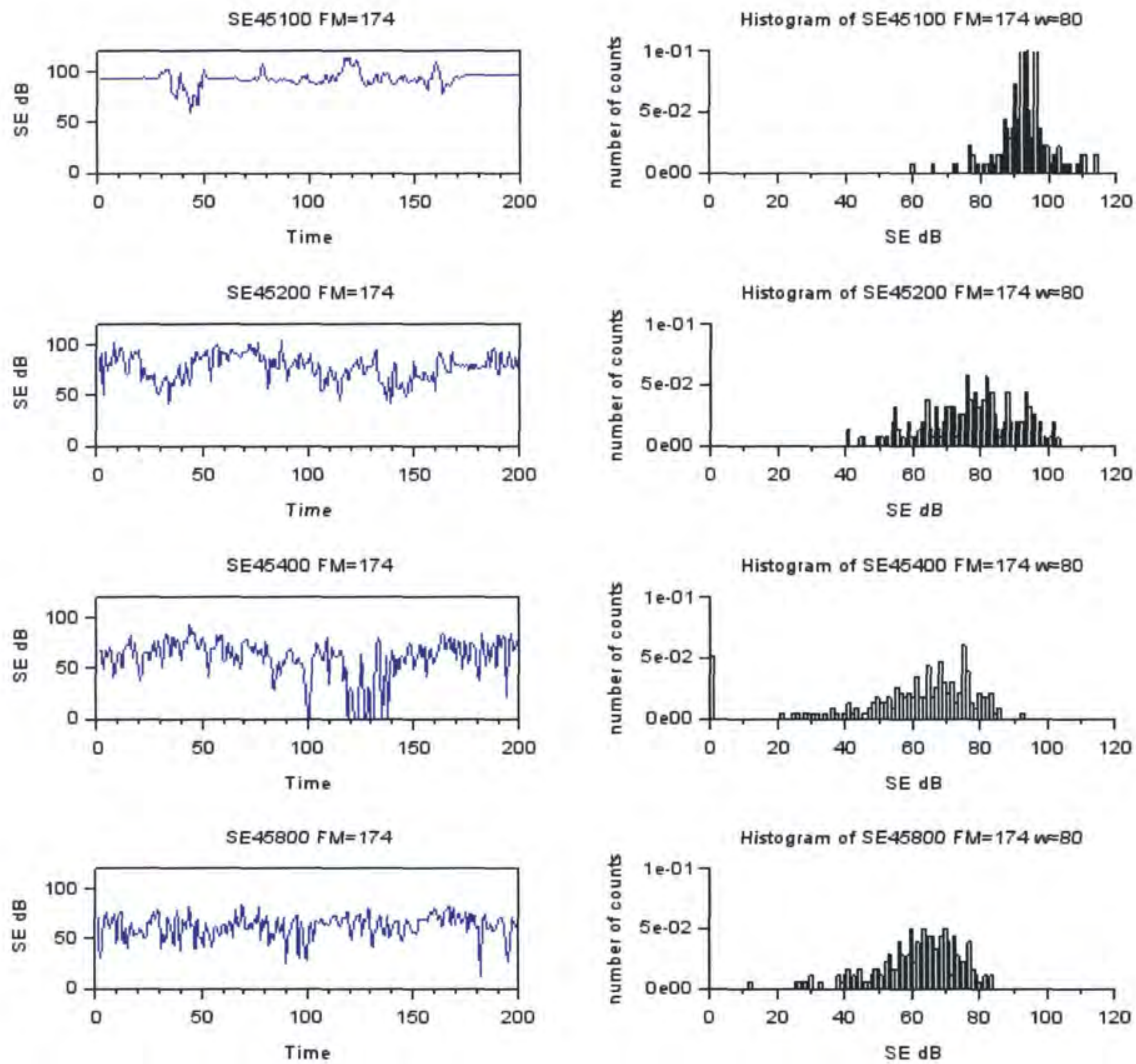

Figure 11. Left Column: Signal Excess (SE) for a target at 45 m depth and source at 50 m depth for 100 m, 200 m, 400 m and 800 m ranges. Right column histogram of SE for the same ranges. FM is the Figure of Merit.

Target Depth 60 m

Source Depth 50 m

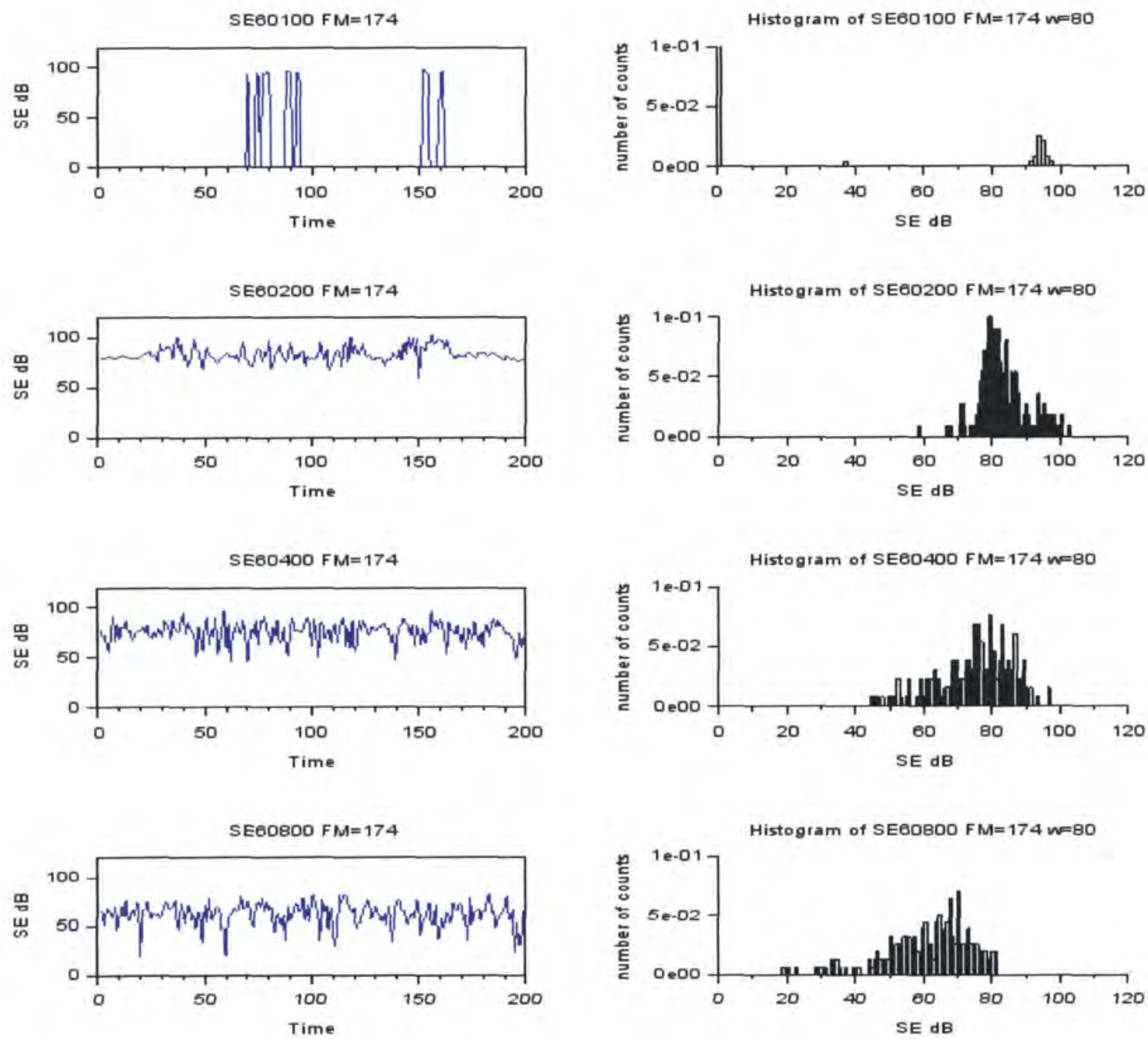

Figure 12. Left Column: Signal Excess (SE) for a target at 60 m depth and source at 50 m depth for 100 m, 200 m, 400 m and 800 m ranges. Right column histogram of SE for the same ranges. FM is the Figure of Merit.

Target Depth 70 m

Source Depth 50 m

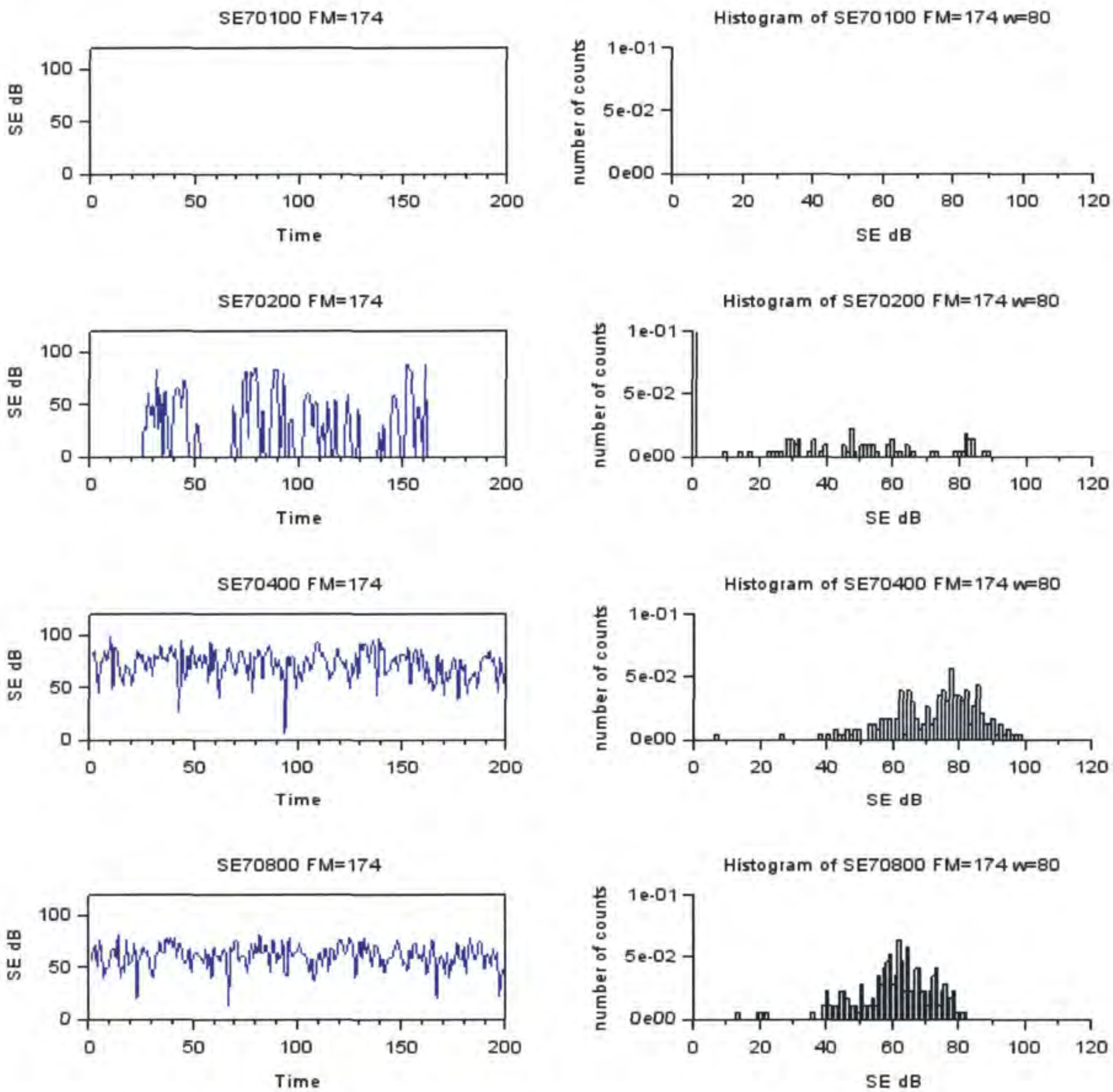

Figure 13. Left Column: Signal Excess (SE) for a target at 70 m depth and source at 50 m depth for 100 m, 200 m, 400 m and 800 m ranges. Right column histogram of SE for the same ranges. FM is the Figure of Merit.

IV. Conclusion

A hypothetical mine detection sonar system's signal excess variability, which was caused by mode 1 internal wave perturbation of the sound speed profile, was calculated for a limited sound speed field time section. Acoustic signals were projected parallel to the propagation direction of the internal wave field. For a sonar system figure of merit equal to 174 dB and at a single source depth, the histograms of the signal excess variability showed the probability distribution of the system response to be target depth and range dependent. The signal excess variability was distributed over 20 dB for short range targets (~200 m) and by more than 60 dB for longer range targets (400 and 800 m), i.e. signal excess histograms showed increased variability with increasing target range. Within the bounds of the calculation, a system operating at 20 kHz and using a projector with a source level of 240 dB re 1μPa @ 1m detected targets with a high % of its pings, see Table I in the FOM=174 column. This was true if the target was in the transducer's primary beam pattern.

However, if the source level of the sonar system was decreased, e.g. to reduce counter detection, the signal excess variability caused by the internal waves resulted in a significant reduction in the % of target detections, see Table I in the columns labeled FOM= 154 to 114 dB. The degradation in the system performance was large enough to call into question its use as a reliable mine detection system.

This signal excess variability study needs to be improved in a number of ways:

1. the impact of source depth on signal excess variability needs to be quantified,

2. longer time sections of the sound speed field for fall oceanographic conditions need to be simulated including intertidal and intra-tidal variability, i.e. spring to neap cycles,
3. seasonal variability of the sound speed profile and its perturbation by the seasonally changing internal wave fields needs to be addressed and
4. acoustic signal propagation studies focused on propagation out of the internal wave plane, in a 3-D sound speed field needs to be performed.
5. an assessment of operational underwater mine hunting tactics needs to be conducted in conjunction with further research. Particular attention should be paid to tactics in regions with known internal wave fields, especially submarine tactics which optimize detectability while minimizing counter detection.
6. optimization of UUV (Unmanned Underwater Vehicles) search, detection, and evaluation algorithms will require further modeling and research of internal waves (refer to point 4.) Incorporating the variability induced by the phenomena is essential to accurate target identification in the littoral region."

---

[1] Orr, Marshall H. and Mignerey, Peter C., "Nonlinear internal waves in the South China Sea: Observation of the conversion of depression internal waves to elevation internal wave", J. Geophysical. Research, *2003*, 108, No. C3, 3064, doi: 10.1029/2001JC001163.

[2] Keenan, R. E. , An introduction to GRAB eigenrays and CASS reverberation and signal excess, OCEANS 2000 MTS/IEEE Conference and Exhibition (Volume:2), *2000*, 1065 -1070, doi: 10.1109/OCEANS.2000.881743

[3] Google Earth.

[4] Godoy, Keenan, and Weinberg, "Express Software Test Description and Introductory User's Guide CASS: Comprehensive Acoustic System Simulation, version 4.3", pg. 6.